

## NUMERICAL STUDY ON THE BOILING HEAT TRANSFER INDUCED BY TWO HEATED PLATES

by

***Xiaopeng SHAN, Geng GUAN, and Deming NIE\****

Institute of Fluid Mechanics, China Jiliang University, Hangzhou, China

Original scientific paper  
<https://doi.org/10.2298/TSCI20S1257S>

*A two-phase lattice Boltzmann method was used to numerically study the boiling heat transfer related to the liquid-vapor transition induced by two heated plates. The effects of the gravity force as well as the separation between the heated plates were examined. The focus is on the bubble departure behavior resulting from the interaction between bubbles, which can be roughly classified into four types of pattern according to the separation between plates. In particular, it is shown that the bubble merging may take place twice in one cycle when the separation is close to a certain value. This is referred to as the pattern of alternation of bubble merging before and after departure, for which a sudden jump is seen in the bubble release period. Furthermore, the heat flux and the flow features are also shown to illustrate the behavior of heat transfer in the present system.*

Key words: *pool boiling, heat transfer, lattice Boltzmann method*

### Introduction

Liquid-vapor phase transition is very common in the process of heat transfer in pool boiling, which is usually characterized by the departure of vapor bubbles at high frequency. Much heat carried by the vapor bubbles will be condensed by the cold liquid after departure. On the other hand, the quiescent liquid is strongly disturbed when the bubbles rise under the action of buoyant force. This may greatly enhance the forced convection by creating a number of re-circulation zones. Due to its high efficiency in heat transfer, pool boiling becomes an important technique of heat removal in many industrial and engineering fields, such as power generation, water purification and air separation.

Over the last decade, the lattice Boltzmann method (LBM) appears as a popular tool for the simulation of multiple-phase flows because of its high ability in dealing with the interface between different phases. A number of lattice Boltzmann models were developed to simulate the boiling heat transfer involving the phase transition, such as the color-gradient model [1], the pseudo-potential model [2], and the free-energy model [3]. Based on these models, much effort has been devoted into the numerical study of heat transfer in the pool boiling. For instance, Dong *et al.* [4] used the LBM to investigate the behavior of bubble growth and departure from a superheated wall. Their results agree with the experimental data from some literatures. Ryu and Ko [5] presented a numerical study on the boiling heat transfer involving a single nucleate site and multiple nucleate sites. A power-law relationship between the Nusselt number and the number of nucleate sites was proposed [5]. Sun and Li [6] studied the bubble departure diameter in pool boiling using a 3-D LBM. They claimed that in the 3-D condition the bubble diameter

\* Corresponding author, e-mail: nieinhz@cjlu.edu.cn

is proportional to  $g^{-0.346}$ , where  $g$  is the acceleration of gravity force. This relation is very close to the one demonstrated by Sadeghi *et al.* [7], *i. e.*  $g^{-0.354}$ . Sun and Li [6] also simulated the phenomenon of two bubbles growth and merging. Based on the pseudo-potential model [2], Gong and Cheng [8] proposed an improved LBM which is shown to have better ability in tracking the liquid-vapor interface. Using this improved LBM the same authors investigated the effects of wettability [9] as well as vapor phase's thermal conductivity [10] on the pool boiling heat transfer. Similar work to [9] was also reported by Li *et al.* [11]. Fang *et al.* [12] presented a 2-D study on the pool boiling with large liquid-vapor density ratio (around 200). Recently, the LBM was used to numerically investigate the enhancement of heat transfer in pool boiling involving a type of hydrophilic-hydrophobic mixed surfaces. According to these studies [13-15], the use of the mixed surface may promote the bubble nucleation and departure, and hence enhance the heat transfer of system under certain conditions. Apart from the lattice Boltzmann simulations, recent efforts [16, 17] were also devoted to developing some theoretical solutions for the heat transfer as well as the fluid-flow.

In comparison with the study on a single nucleate site, much more attention should be paid to the boiling heat transfer involving bubble interactions, which is the general case in the engineering and industrial applications. When there are two or more nucleate sites in the pool boiling, the interaction between vapor bubbles may be significant in the process of heat transfer. For instance, the bubble merging may take place under certain conditions, which has a noticeable influence on the bubble departure diameter as well as on the bubble release frequency. Furthermore, once a bubble departs from the nucleate site the flow disturbance is always seen, which may accelerate or decelerate the growth and departure of other bubbles. This is known as the hydrodynamic interactions, leading to a strong coupling between the heat transfer and the fluid-flow. This makes a pool boiling system more complex. Literature survey shows that the pooling boiling involving bubble interactions is far from well understood. This motivates the present work.

### Two-phase lattice Boltzmann method

In this work we use the two-phase LBM proposed by Gong and Cheng [8] to solve the flow and temperature fields, which is briefly introduced here. The lattice Boltzmann equations,  $f_i$ , for the fluid density,  $\rho$ , and velocity,  $\mathbf{u}$ , are expressed:

$$f_i(\mathbf{x} + \mathbf{e}_i \Delta t, t + \Delta t) - f_i(\mathbf{x}, t) = -\frac{1}{\tau_f} [f_i(\mathbf{x}, t) - f_i^{(eq)}(\mathbf{x}, t)] + \Delta f_i \quad (1)$$

where  $f_i(\mathbf{x}, t)$  is the density distribution function corresponding to the microscopic velocity  $\mathbf{e}_i$ ,  $\Delta t$  – the time step of the simulation,  $\tau_f$  – the relaxation time, and  $f_i^{(eq)}(\mathbf{x}, t)$  – the equilibrium distribution function which is given:

$$f_i^{(eq)} = w_i, \rho \left[ 1 + \frac{\mathbf{e}_i \cdot \mathbf{u}}{c_s^2} + \frac{(\mathbf{e}_i \cdot \mathbf{u})^2}{2c_s^4} - \frac{\mathbf{u}^2}{2c_s^2} \right] \quad (2)$$

where  $c_s$  is the speed of sound, and  $w_i$  are weights related to the lattice model. The  $\Delta f_i$  is the discrete form of the body force  $\mathbf{F}$  [8], which accounts for the inter-particle interaction force  $\mathbf{F}_{int}$  [8], the gravitational force  $\mathbf{F}_g$  and the interaction force between solid surface and fluid  $\mathbf{F}_s$ . The fluid density and velocity are obtained through:

$$\rho = \sum_i f_i, \rho \mathbf{u} = \sum_i \mathbf{e}_i f_i \quad (3)$$

Due to the forcing term [8], the real fluid velocity of fluid  $\mathbf{U}$  is modified:

$$\rho \mathbf{U} = \sum_i \mathbf{e}_i f_i + \frac{\Delta t}{2} \mathbf{F} \quad (4)$$

Similarly, another set of lattice Boltzmann equations,  $g_i$ , are proposed [8] to solve the temperature field of fluid,  $T$ , which are given:

$$g_i(\mathbf{x} + \mathbf{e}_i \Delta t, t + \Delta t) - g_i(\mathbf{x}, t) = -\frac{1}{\tau_g} [g_i(\mathbf{x}, t) - g_i^{(eq)}(\mathbf{x}, t)] + \Delta t w_i \phi \quad (5)$$

where  $\tau_g$  is the relaxation time for the fluid temperature and  $g_i^{(eq)}(\mathbf{x}, t)$  is the corresponding equilibrium distribution function:

$$g_i^{(eq)} = w_i T \left[ 1 + \frac{\mathbf{e}_i \cdot \mathbf{U}}{c_s^2} + \frac{(\mathbf{e}_i \cdot \mathbf{U})^2}{2c_s^4} - \frac{\mathbf{U}^2}{2c_s^2} \right] \quad (6)$$

The source term  $\phi$  is responsible for the phase change, determined:

$$\phi = T \left[ 1 - \frac{1}{\rho c_v} \left( \frac{\partial p}{\partial T} \right)_\rho \right] \nabla \cdot \mathbf{U} \quad (7)$$

where  $p$  is the pressure and  $c_v$  is the heat capacity. Then the temperature is obtained:

$$T = \sum_i g_i \quad (8)$$

In order to account for the pressure involving phase transition, the Peng-Robinson (P-R) equation of state [18] was adopted here.

Note that for both  $f_i$  and  $g_i$ , the 9-velocity model in two dimensions (*i. e.* D2Q9) is used here, which has the following discrete velocity vectors:

$$\mathbf{e}_i = \begin{cases} (0, 0), & \text{for } i = 0 \\ (\pm 1, 0)c, (0, \pm 1)c & \text{for } i = 1 \text{ to } 4 \\ (\pm 1, \pm 1)c, & \text{for } i = 5 \text{ to } 8 \end{cases} \quad (9)$$

where  $c = \Delta x / \Delta t$  is the lattice speed and  $\Delta x$  is the lattice space. For simplicity, both the lattice space and the time step are set to be 1 in the simulations, *i. e.*  $\Delta x = \Delta t = 1$ .

### Problem description and validation

This work aims to numerically study the behavior of boiling heat transfer induced by two nucleate sites, *i. e.* two heated plates. The focus is on the interaction between two vapor bubbles. Figure 1 shows the physical geometry of the problem. The liquid of density,  $\rho_s$ , and temperature,  $T_s$ , is filled with in a 2-D domain with dimensions  $L \times H$ . Two heated plates of length,  $L_h$ , and temperature  $T_h$  ( $T_h > T_s$ ) are symmetrically placed on the bottom wall. The separation between the plates is denoted as  $L_d$ . For the upper boundary, a constant pressure is always maintained. In doing so, the saturated pressure is firstly computed

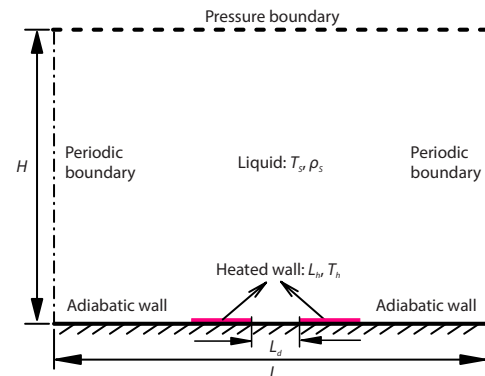
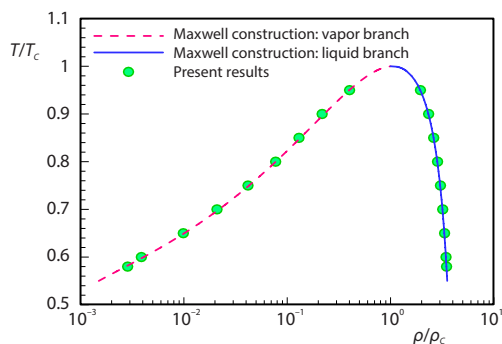


Figure 1. Physical geometry and notations used in the present problem

through the P-R equation using both values of  $\rho_s$  and  $T_s$ . Then, the unknown distribution functions on the upper boundary are determined through the non-equilibrium bounce-back scheme. The periodic boundary conditions are employed in the horizontal direction. In the simulations, the parameters are fixed  $L = 300$ ,  $H = 600$ ,  $L_h = 10$ , and  $T_h = 0.98T_c$ . The temperature of the saturated liquid is chosen as  $T_s = 0.9T_c$  ( $T_c$  is the critical temperature of the liquid), which corresponds to the coexistence densities  $\rho_L \approx 2.324 \rho_c$  and  $\rho_G \approx 0.228 \rho_c$  (i. e.  $\rho_L/\rho_G \approx 10$ ). Note that  $\rho_L$  and  $\rho_G$  are the densities of the liquid and the vapor, respectively,  $\rho_c$  denotes the critical density of the liquid. It should be stated here that the parameters are all in lattice units, which is very common in the lattice Boltzmann simulations.



**Figure 2.** Comparison of the coexistence curves obtained from the present computations and the analytical solution (i. e. Maxwell construction theory)

and  $\rho/\rho_c > 1$  represent the vapor phase and liquid phase, respectively. Furthermore, the liquid/vapor density ratio can be higher than 1000 for the P-R EOS.

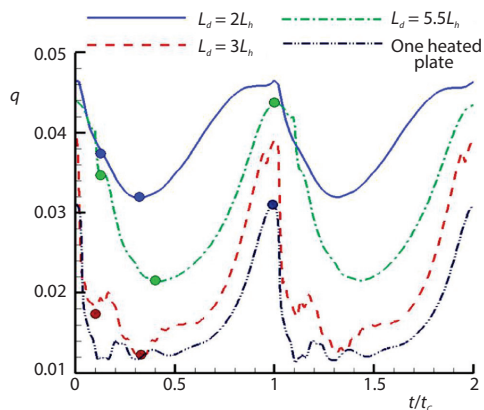


**Figure 3.** Time history of the heat flux,  $q$ , averaged over the heated plates for different separations between them during two periods: note that  $t_c$  is the time period of bubble departure; to provide a direct comparison the corresponding result for a single heated plate is also shown

In order to validate our computational code, the liquid-vapor coexistence curve obtained from our computations is compared with the theoretical curve predicted by the Maxwell construction theory, which is given by fig. 2. In thermodynamics, the coexistence curve, also known as binodal curve, denotes the condition at which two distinct phases may coexist. Equivalently, it is the boundary between the set of conditions in which it is thermodynamically favorable for the system to be fully mixed and the set of conditions in which it is thermodynamically favorable for it to phase separate. As can be seen from fig. 2, our results agree well with the theoretical values. Note that  $\rho/\rho_c < 1$

## Numerical results

As shown in fig. 3, the separation between the heated plates,  $L_d$ , has a strong effect on the heat flux  $q$  (i. e.). Note that  $q$  is averaged over the two plates, which is given:

$$q = - \int_{\text{heated plates}} \lambda \frac{\partial T}{\partial y} dx \quad (10)$$

where  $\lambda$  is the thermal conductivity which is fixed at 1 for the sake of simplicity. In fig. 3  $t_c$  is the time period of bubble departure.

Three representative values of  $L_d$  are considered. For the purpose of comparison, the heat flux of a single heated plate is also presented in fig. 3. It is clearly shown that the heat flux is always larger for the case of two heated plates irrespective of the separation between them. However, as  $L_d$  increases the heat flux decreases firstly, then increases. The possible mechanism is discussed in the following.

Figure 4 shows the instantaneous flow fields and the density contours at different times during one period to illustrate the process of bubble growth and departure. The separation between the plates is  $L_d = 2L_h$ . It is seen that only one bubble is generated due to the pool boiling. The two heated plates are so close that the bubbles merge into a bigger one on the wall. As a consequence, the general feature for  $L_d = 2L_h$  is similar to that for a single heated plate. By contrast, two bubbles are clearly seen on the wall if increasing the separation between the two plates, *e. g.*  $L_d = 3.5L_h$  as shown in fig. 5. Interestingly, the two bubbles come close to each other as they grow, fig. 5(c), which eventually merge into a larger one before departure, fig. 5(d). In particular, it can be seen that the residual part of bubble on the wall is nearly condensed by the liquid, as shown in fig. 5(a), which is largely responsible for the decrease of heat flux as shown in fig. 3. Another consequence of this behavior is the remarkable increasing period of bubble release, as one can see in fig. 6. The main reason behind this phenomenon is that the process of bubble growth and departure needs a long time when there is little residual bubble on the plates.

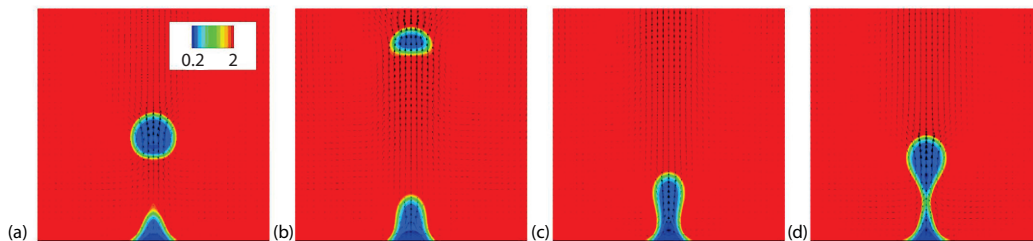


Figure 4. Instantaneous flow fields and density contours at different times for  $L_d = 2L_h$  illustrating the process of bubble growth and departure during one period (bubble merging on the wall); (a)  $t = 1/8t_c$ , (b)  $t = 1/2t_c$ , (c)  $t = 3/4t_c$ , and (d)  $t = t_c$

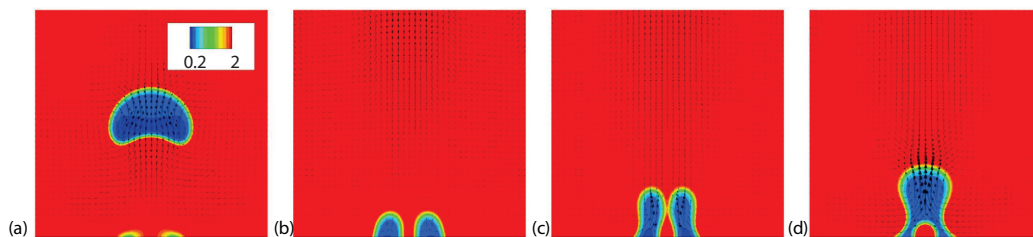


Figure 5. Instantaneous flow fields and density contours at different times for  $L_d = 3.5L_h$  illustrating the process of bubble growth and departure during one period (bubble merging before departure); (a)  $t = 1/10t_c$ , (b)  $t = 3/5t_c$ , (c)  $t = 9/10t_c$ , and (d)  $t = t_c$

When the two heated plates are far away from each other, such as  $L_d = 5.5L_h$ , no bubble merging can be seen, as shown in fig. 7. The bubbles are rising separately after they depart from the wall. Even so, the interaction between them is still significant in terms of the bubble departure diameter as well as the fluid velocity. Moreover, in comparison with  $L_d = 3.5L_h$ , fig. 5, the bubble release period is seen to apparently decrease.

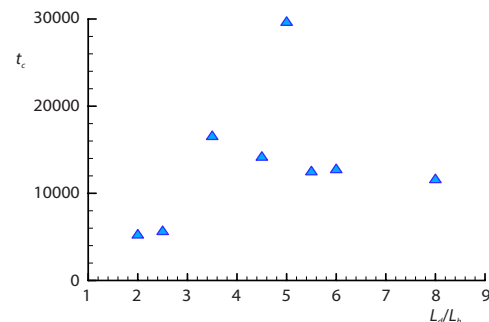
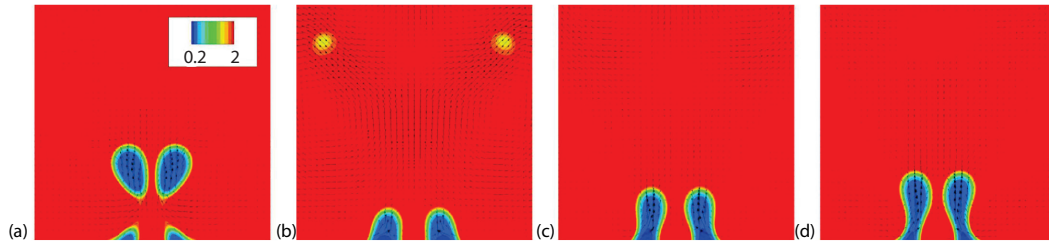
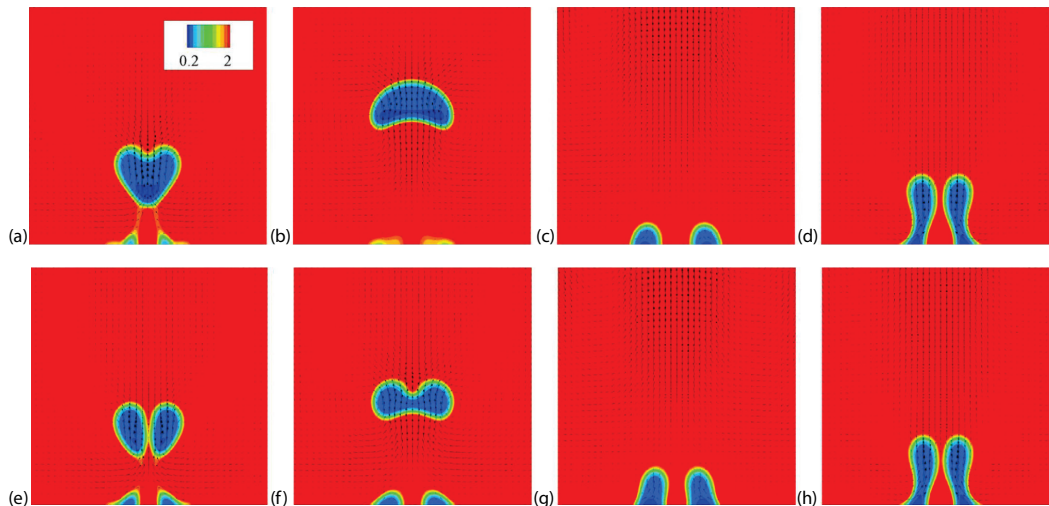


Figure 6. Dependence of the time period of bubble release,  $t_c$ , on the separation of the heated plates ( $L_d/L_h$ )



**Figure 7. Instantaneous flow fields and density contours at different times for  $L_d = 5.5L_h$  illustrating the process of bubble growth and departure during one period (bubble rising separately); (a)  $t = 1/8t_c$ , (b)  $t = 5/8t_c$ , (c)  $t = 7/8t_c$ , and (d)  $t = t_c$**

It is interesting to find a unique pattern of liquid-vapor phase change in the present system when the separation between the plates is close to  $5L_h$ , as shown in fig. 8. The bubble merging occurs twice during one period of cycle. As one can see in fig. 8(a), the bubbles merge into a larger one before they depart from the wall, which is similar to fig. 5 (*i. e.*  $L_d = 3.5L_h$ ). However, the next bubble merging takes place after the bubbles depart, fig. 8(d)-8(f). The process is repeated, leading to an alternation of the bubble merging before and after departure. The effects of this unique pattern on the bubble release period, fig. 6, and the heat flux, fig. 9, are significant. It is clearly seen that there are two peaks in the heat flux during one period, corresponding to the alternation of the bubble merging. The most striking observation is the sudden jump in the bubble release period, as shown in fig. 6, which is almost twice that seen at  $L_d = 4.5L_h$  or  $L_d = 5.5L_h$ .



**Figure 8. Instantaneous flow fields and density contours at different times for  $L_d = 5L_h$  illustrating the process of bubble growth and departure during one period (alternation of the bubble merging before and after departure): (a)  $t = 1/20t_c$ , (b)  $t = 1/10t_c$ , (c)  $t = 3/10t_c$ , (d)  $t = 3/5t_c$ , (e)  $t = 5/8t_c$ , (f)  $t = 2/3t_c$ , (g)  $t = 7/8t_c$  and (h)  $t = t_c$**

In order to provide a better understanding of the heat transfer involving two nucleate sites, fig. 10 shows the instantaneous contours of the vertical component of fluid velocity for  $L_d = 2L_h$  and  $L_d = 5.5L_h$ , respectively. The results are chosen at the times when the heat flux reaches its maximum. For the purpose of comparison, the corresponding result for the case

of a single heated plate is also presented. As shown in fig. 10(a), the two plates are so close that there is only one large bubble departing from the wall, which results in a much stronger upward stream as compared with the case of a single heated plate, fig. 10(c). This greatly enhances the forced convection between the heated plates and the cold liquid and improves the rate of heat transfer in the pool boiling, in consistent with fig. 3. When the two plates are far away from each other, *e. g.*  $L_d = 5.5L_h$ , as shown in fig. 10(b), two upward streams are generated due to the heated plates, which gives rise to strong flow disturbance by creating multiple re-circulation zones. This can also be viewed as a consequence of the hydrodynamic interactions. The performance of heat transfer may be illustrated by fig. 11, which shows the instantaneous fluid temperature corresponding to each case shown in fig. 10. In comparison with the case of a single heated plate, much more heat is delivered into the cold liquid and eventually dissipated for the case of two heated plates by considering the area of the hot fluid which is going up as well as that of the cold fluid close to the heated plates, as shown in fig. 11.

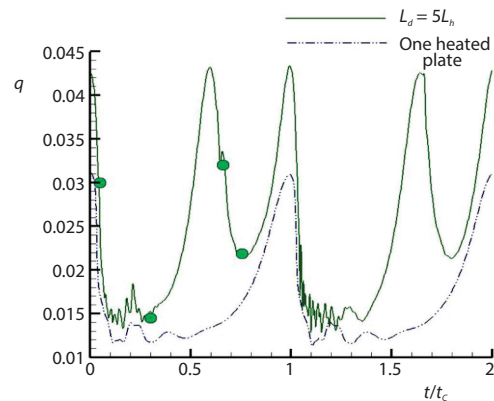


Figure 9. Time history of the averaged heat flux,  $q$ , for  $L_d = 5L_h$  during two periods along with the corresponding result of a single heated plate

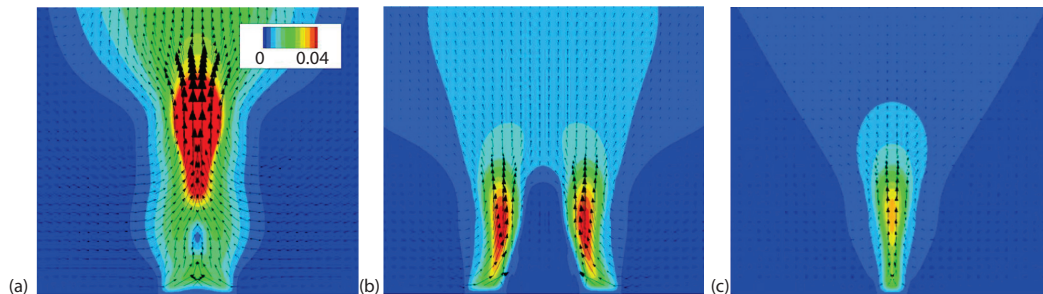


Figure 10. Instantaneous contours of the vertical component of fluid velocity at the time when the heat flux,  $q$ , reaches its maximum for the cases of (a) two heated plate at  $L_d = 2L_h$ , (b) two heated plate at  $L_d = 5.5L_h$ , and (c) a single heated plate

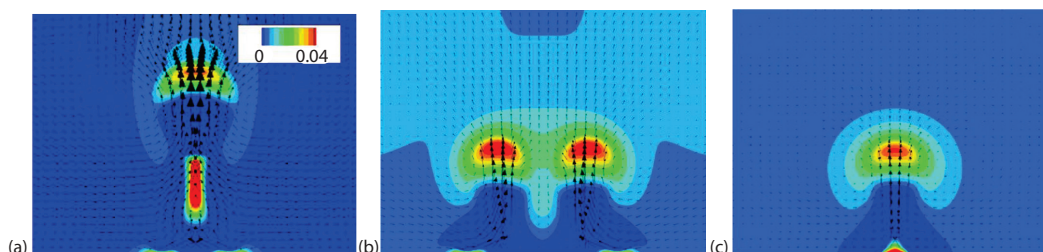
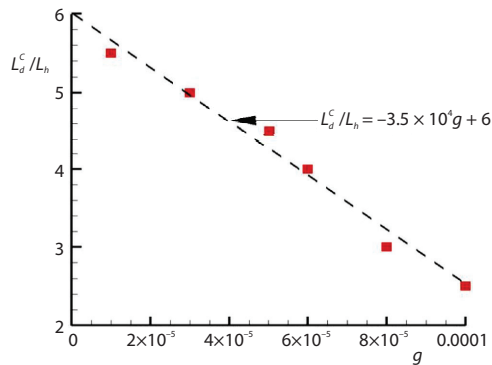


Figure 11. Instantaneous contours of the fluid temperature  $[(T-T_s)/T_c]$  at the same time as fig. 10

Finally, our focus moves to the pattern of bubble merging on the wall (*i. e.* fig. 4). As aforementioned, there is only one large bubble when the nucleate sites are close enough



**Figure 12. Dependence of the critical separation ( $L_d^c/L_h$ ) (below which the bubbles merge on the wall) on the gravity force,  $g$**

to each other. In this situation the heat transfer is enhanced in terms of both the heat flux and the bubble release frequency, which is significant for the engineering applications involving a cooling system. Figure 12 shows the influence of the gravity force on this pattern. The normalized critical separation, *i. e.*  $L_d^c/L_h$ , below which the bubbles merge on the wall, is seen to linearly decrease with the gravity force. This could be explained as follows. As the gravity force increases, the buoyant effects become strong. If the heated plates are too far from each other, the bubbles may depart from the wall separately before they merge.

### Conclusion

In this work a two-phase LBM was used to numerically study the behavior of heat transfer involving the liquid-vapor transition in pool boiling induced by two heated plates. Much attention has been paid to the interaction between vapor bubbles. It is shown that the heat transfer is greatly enhanced as compared with the case of a single heated plate in terms of the heat flux as well as the bubble release frequency. Roughly speaking, four types of bubble departure patterns have been identified according to the separation between the plates, *i. e.* bubble merging on the wall, bubble merging before departure, alternation of bubble merging before and after departure and bubble rising separately. When the plates are very close to each other, the bubbles merge into a larger one before departure, which is referred to as the pattern of bubble merging on the wall. This pattern is characterized by its large heat flux and high bubble release frequency. In addition, the critical separation for this pattern is shown to linearly decrease with the gravity force. In particular, there is a sudden jump in the bubble release period when the separation is close to a certain value (*i. e.* five times the length of heated plate) because the bubble merging occurs twice in one cycle. This is the pattern of alternation of bubble merging before and after departure.

### Acknowledgment

This work was supported by the National Key Research and Development Program of China (2017YFB0603700) and the National Natural Science Foundation of China (Grants 11972336).

### Reference

- [1] Gunstensen, A. K., *et al.*, Lattice Boltzmann Model of Immiscible Fluids, *Physical Review A*, 43 (1991), 8, pp. 4320-4327
- [2] Shan, X., Chen, H., Lattice Boltzmann Model for Simulating Flows with Multiple Phases and Components, *Physical Review E*, 47 (1993), 3, pp. 1815-1820
- [3] Swift, M. R., *et al.*, Lattice Boltzmann Simulations of Liquid-Gas and Binary Fluid Systems, *Physical Review E*, 54 (1996), 5, pp. 5041-5052
- [4] Dong, Z., *et al.*, A Numerical Investigation of Bubble Growth on and Departure from a Superheated Wall by Lattice Boltzmann Method, *International Journal of Heat and Mass Transfer*, 53 (2010), 21-22, pp. 4908-4916
- [5] Ryu, S., Ko S., Direct Numerical Simulation of Nucleate Pool Boiling Using a 2-D Lattice Boltzmann Method, *Nuclear Engineering and Design*, 248 (2012), July, pp. 248-262

- [6] Sun, T., Li, W., The 3-D Numerical Simulation of Nucleate Boiling Bubble by Lattice Boltzmann Method, *Computers and Fluids*, 88 (2013), Dec., pp. 400-409
- [7] Sadeghi, R., *et al.*, A 3-D Lattice Boltzmann Model for Numerical Investigation of Bubble Growth in Pool Boiling, *International Communications in Heat and Mass Transfer*, 79 (2016), Dec., pp. 58-66
- [8] Gong, S., Cheng, P., A Lattice Boltzmann Method for Simulation of Liquid-Vapor Phase-Change Heat Transfer, *International Journal of Heat and Mass Transfer*, 55 (2012), 17-18, pp. 4923-4927
- [9] Gong S., Cheng P., Lattice Boltzmann Simulations for Surface Wettability Effects in Saturated Pool Boiling Heat Transfer, *International Journal of Heat and Mass Transfer*, 85 (2015), June, pp. 635-646
- [10] Gong S., Cheng P., Direct numerical simulations of pool boiling curves including heater's thermal responses and the Effect of Vapor Phase's Thermal Conductivity, *International Communications in Heat and Mass Transfer*, 87 (2017), Oct., pp. 61-71
- [11] Li, Q., *et al.*, Lattice Boltzmann Modelling of Boiling Heat Transfer: The Boiling Curve and the Effects of Wettability, *International Journal of Heat and Mass Transfer*, 85 (2015), June, pp. 787-796
- [12] Fang, W. Z., *et al.*, Lattice Boltzmann Modelling of Pool Boiling with Large Liquid-Gas Density Ratio, *International Journal of Thermal Sciences*, 114 (2017), Apr, pp. 172-183
- [13] Yu, Y., *et al.*, Boiling Heat Transfer on Hydrophilic-Hydrophobic Mixed Surfaces: A 3-D Lattice Boltzmann Study, *Applied Thermal Engineering*, 142 (2018), Sept., pp. 846-854
- [14] Li, Q., *et al.*, Enhancement of Boiling Heat Transfer Using Hydrophilic-Hydrophobic Mixed Surfaces: A Lattice Boltzmann Study, *Applied Thermal Engineering*, 132 (2018), Mar., pp. 490-499
- [15] Ma, X., *et al.*, Simulations of Saturated Boiling Heat Transfer on Bioinspired Two-Phase Heat Sinks by a Phase-Change Lattice Boltzmann Method, *International Journal of Heat and Mass Transfer*, 127 (2018), Part B, pp. 1013-1024
- [16] Kilicman, A., *et al.*, Analytic Approximate Solutions for Fluid-Flow in the Presence of Heat and Mass Transfer. *Thermal Science*, 22 (2018), Suppl. 1, pp. S259-S264
- [17] Partohaghighi, M., *et al.*, Fictitious Time Integration Method for Solving the Time Fractional Gas Dynamics Equation. *Thermal Science*, 23 (2019), Suppl. 6, pp. S2009-S2016
- [18] Yuan, P., Schaefer, L., Equations of State in a Lattice Boltzmann Model, *Physics of Fluids*, 18 (2006), 042101